(^{16}O, ^{15}N) Reaction on $2s$-$1d$- and $1f$-$2p$-Shell Nuclei*

J. V. Maher, K. A. Erb, and R. W. Miller
Nuclear Physics Laboratory, University of Pittsburgh, Pittsburgh, Pennsylvania

(Received 5 June 1972)

The (^{16}O, ^{15}N) reaction has been studied on targets of ^{24}Mg, ^{27}Al, ^{28}Si, ^{45}Sc, and ^{46,48}Ti and finite-range distorted-wave calculations have accounted well for the extreme Q dependences (arising from angular momentum mismatch) of the cross sections, yielding spectroscopic factors in good agreement with spectroscopic factors extracted from light-ion-induced reactions. This agreement is interpreted as an indication that the heavy-ion-induced proton transfer reaction – when it populates states of strong single-particle character – can be well understood within the framework of the distorted-wave theory.

I. INTRODUCTION

Not only is an understanding of the interactions of complex projectiles with heavy targets of intrinsic interest, but the extension of present knowledge of nuclear systematics to nuclides far from the stability line requires the use of reactions initiated by heavy projectiles. However, the lack of a systematic body of experimental information and the theoretical complexity of the situation have combined to prevent a thorough understanding of such reactions at present. With the partial solution of several formidable experimental problems much attention has recently been focused on the systematic accumulation of heavy-ion transfer reaction data.[1-4] If these reactions are to exhibit empirical simplicity, it might be revealed in studies which cover a large mass region. In this paper we report the results of a study of the (^{16}O, ^{15}N) reaction on several targets in the $2s$-$1d$ and $1f$-$2p$ shells. The primary purpose of the study was not to investigate the (^{16}O, ^{15}N) reaction as a spectroscopic tool and alternative to the (^{3}He, d) reaction, but rather to learn which comparisons can be made between one-proton-transfer reactions induced by light and heavy projectiles as a first step in proceeding to studies of large cluster transfers. Although multinucleon-transfer data were measured simultaneously with the single-proton-transfer data and reports of some of the multinucleon-transfer results have been presented,[1] only the (^{16}O, ^{15}N) results are presented in this paper.

II. EXPERIMENTAL METHOD

The reactions studied in this work were investigated as functions of angle and energy. The ^{16}O beam from the Pittsburgh three-stage Van de Graaff was typically 1.5 μA in the 6^+ charge state ($\leq$48 MeV) and 0.5 μA in the 7^+ charge state (up to 53 MeV). Targets of ^{27}Al, ^{45}Sc and enriched ^{24}Mg, ^{28}Si, ^{46}Ti, and ^{48}Ti were made by evaporation of ~50 μg/cm^2 of metal on a thin (10- or 20-μg/cm^2) carbon backing. Emerging particles were detected in two ΔE-E detector telescopes (each consisting of a planar Au-Si surface barrier detector ~9 μ thick in front of a 50-μ Au-Si surface-barrier detector). Target thickness and kinematic factors (determined by beam divergence and detector collimator width) were chosen to give approximately equal contributions to a typical over-all energy resolution of ~250 keV.

The telescopes were set 20° apart and a laboratory angle range from 20 to 60° was typically studied. For each telescope, signals from the ΔE and E detectors were summed and the ΔE and summed signals were processed by parallel analog-to-digital converters (ADC's). (During the earlier phase of this experiment, a fixed-wire Nuclear Data analyzer was used. This was later replaced by a Tennelec Pace 4 system interfaced to a PDP 15-40 on-line computer.) The ADC signals were stored event by event on magnetic tape and were subsequently sorted into 256×128-channel arrays. Energy spectra for individual residual chemical elements were extracted from the two-dimensional arrays. It has not been possible to determine the ability of the telescope to separate nitrogen isotopes because in all cases studied there has been no evidence for population of any states of ^{14}N. Differences in the kinematic behavior of ^{14}N and ^{15}N over the angular range studied are sufficiently large compared with the over-all energy resolution discussed above that it has been possible to identify every state discussed below as arising from the (^{16}O, ^{15}N) reaction.

A monitor detector was set at $\theta = -38°$ to check for target deterioration effects. Since in every case elastic scattering events were measured simultaneously with reaction events and since each target was studied at some energy-angle combination where the elastic scattering is believed to be

pure Rutherford scattering, absolute cross sections reported below are expected to be accurate to ±20%.

III. DATA PRESENTATION

Spectra for the (^{16}O, ^{15}N) reaction on targets of ^{27}Al, ^{45}Sc, ^{46}Ti, and ^{48}Ti are shown in Figs. 1 and 2. This reaction is clearly highly selective and details of this selectivity will be discussed below. Beam energies for the angular distribution studies were chosen after excitation functions ($\theta_{lab} \cong 30°$) had been measured in 2-MeV steps from 36–52 MeV for Al and from 40–52 MeV for Ti. The ^{27}Al(^{16}O, ^{15}N) reaction populating the ground state and the 1.779-MeV state of ^{28}Si had previously been studied by Newman, Toth, and Zucker[5] at energies up to 36 MeV. Their results showed that

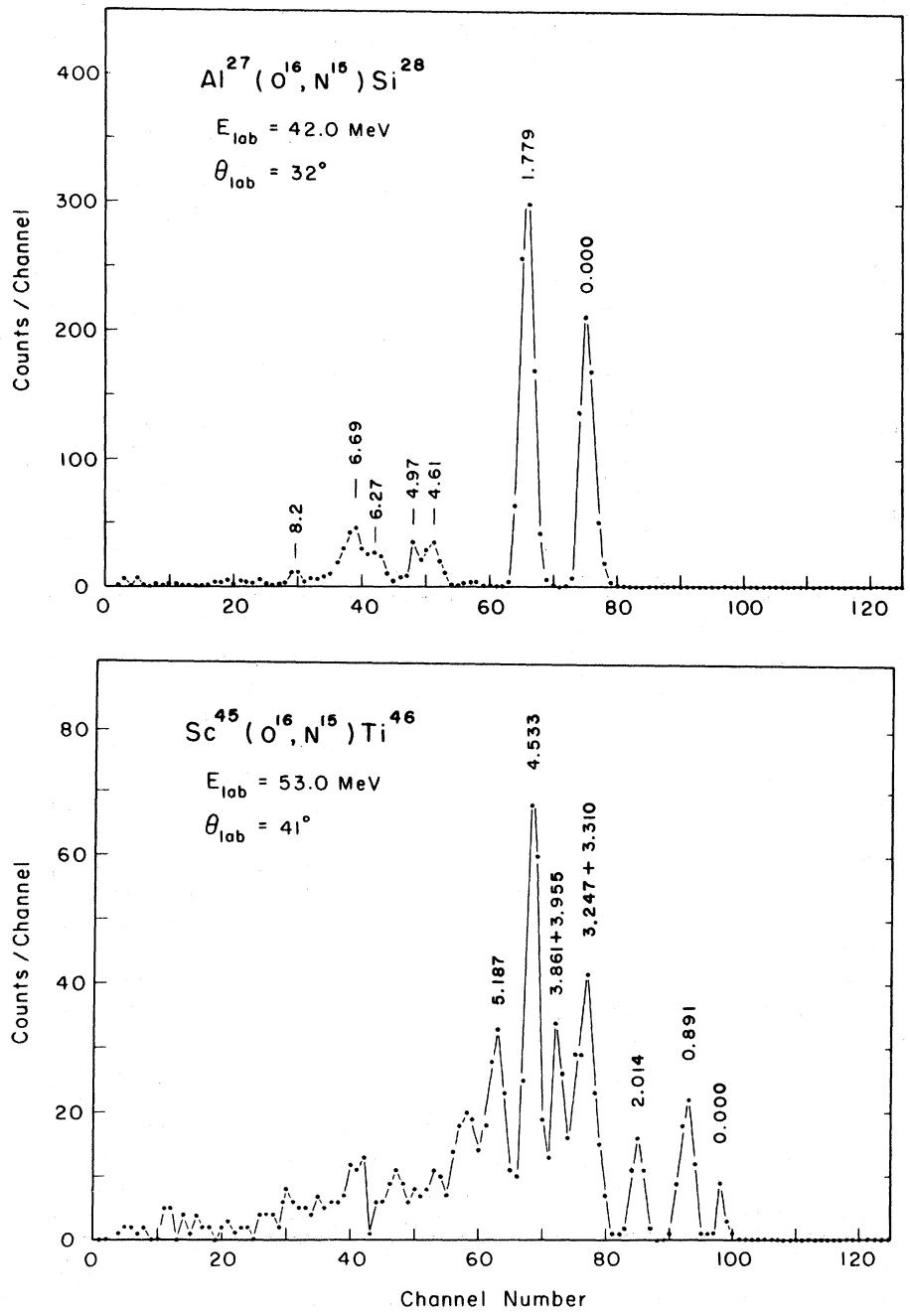

FIG. 1. ^{27}Al(^{16}O, ^{15}N)^{28}Si and ^{45}Sc(^{16}O, ^{15}N)^{46}Ti spectra.

the peak cross sections rise rapidly with beam energy in the neighborhood of the Coulomb barrier. The present study agrees well with the previous result at 36 MeV but shows that, as energy is increased further above the Coulomb barrier, the peak cross section does not change rapidly. This is illustrated in Fig. 3 where ^{27}Al(^{16}O, ^{15}N)^{28}Si angular distributions are shown for several states and several beam energies. In each case, the angle of the peak cross section decreases with increasing beam energy – as would be expected from simple diffraction theories[6] and also from the distorted-wave approach to be discussed below.

The ^{16}O + ^{48}Ti and ^{16}O + ^{45}Sc systems are close to the Coulomb barrier in the energy region between 40 and 50 MeV and appear to reach their peak proton-transfer cross sections at $E_{lab} \simeq 50$ MeV. All the above considerations led to the following choic-

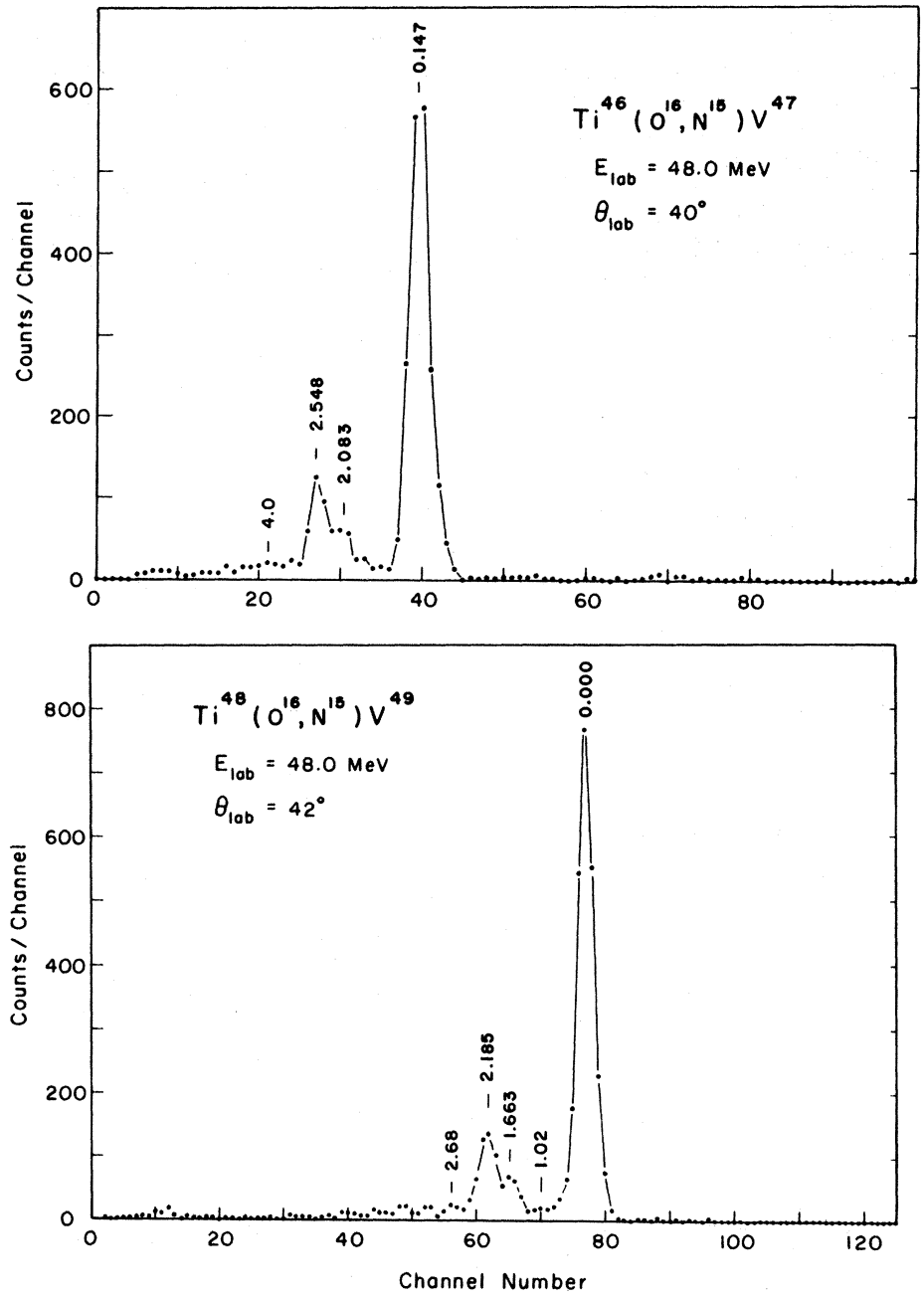

FIG. 2. ^{46,48}Ti(^{16}O, ^{15}N)^{47,49}V spectra.

es of beam energies: Mg-Al-Si targets were studied at $E_{lab} = 42$ MeV where the peak cross section occurs at an easily accessible ($\theta > 20°$) lab angle. ^{46,48}Ti were studied at 48 MeV where the peak cross section is very close to its maximum value and where the ~1.5-μA 6^+ oxygen beam could be exploited. Since, even with the use of a target vibrator, the Sc targets could not withstand more than ~250 nA of beam, Sc was studied with the 53-MeV 7^+ oxygen beam.

Figure 4 shows angular distributions for transitions populating ^{28}Si states through the ^{27}Al(^{16}O, ^{15}N) reaction. The shapes of the angular distributions are very uniform and insensitive to the spectroscopic properties of the final state. Relative peak cross sections are highly sensitive to angular momentum matching as will be discussed below. Figure 5 shows angular distributions for transitions populating ^{49}V states through the ^{48}Ti(^{16}O, ^{15}N) reaction. Again, the three strong states show uniform shapes but strongly varying peak cross sections. The weak states are not believed populated through direct processes as will be discussed below. Figure 6 shows angular distributions for transitions to ^{46}Ti states populated in the ^{45}Sc(^{16}O, ^{15}N) reaction. Angular distributions for (^{16}O, ^{15}N) transitions exciting states in ^{47}V are shown in Fig. 7. The ^{24}Mg(^{16}O, ^{15}N)^{25}Al and ^{28}Si(^{16}O, ^{15}N)^{29}P reactions did not populate any states strongly.

IV. DISTORTED-WAVE ANALYSIS AND DISCUSSION

The distorted-wave calculations in this study were performed with the code RDRC.[7] This code allows proper finite-range treatment of the form factors for the (assumed $1p_{1/2}$) proton bound in the ^{16}O projectile and for the stripped proton in the final nucleus. The code ignores recoil effects. A recent study has shown recoil effects to be important for ^{208}Pb + ^{16}O sub-Coulomb stripping.[8] This study indicates that such effects may be more pronounced for heavy targets than for light targets.[8] Since the results of the calculations dis-

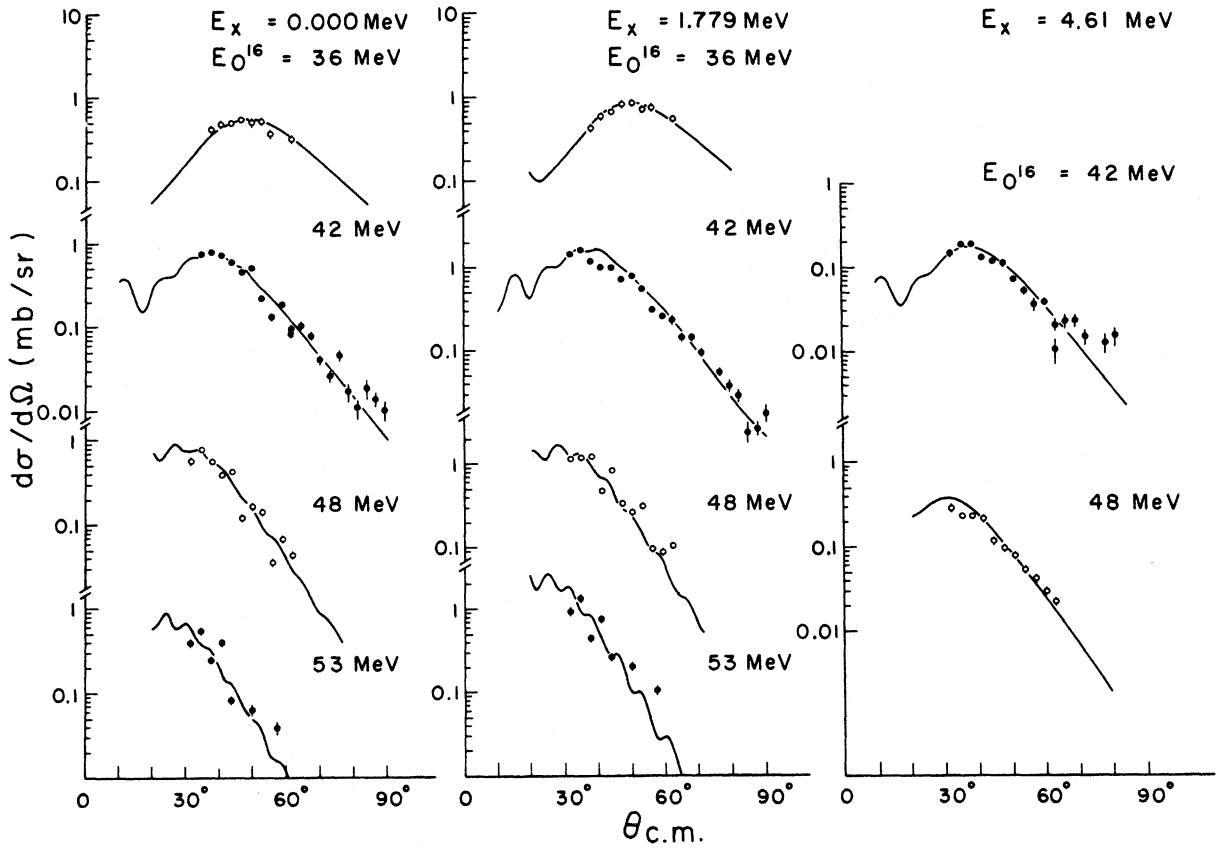

FIG. 3. Selected ^{27}Al(^{16}O, ^{15}N)^{28}Si angular distributions obtained at $E_{^{16}O} = 36$, 42, 48, and 53 MeV. The curves are the results of DWBA calculations using potential set A of Table I.

cussed below yield good agreement with results of (^{3}He, d) studies, it is possible that recoil effects for the (^{16}O, ^{15}N) transitions considered in this work are relatively constant and can be absorbed in the over-all normalization factor discussed below.

Several optical potential parameter sets were used in this study. Since the intention in this work was not to extract spectroscopic factors for the already well studied states we populate, but rather to test the ability of the reaction theory to predict systematics of the reaction mechanism, it was considered important to investigate possible sensitivity to choice of optical parameters – particularly since heavy-ion optical potentials are considerably less well established than those used for light ions. Parameters for the optical potentials studied are listed in Table I. Sets A for ^{16}O and ^{15}N are those which Morrison *et al.* have found to give excellent results in their study of the (^{16}O, ^{15}N) reaction on 1f-2p-shell nuclei.[2] These are very similar to the potentials used by Voos, von Oertzen, and Bock[9] for 1p-shell targets so no additional potentials from the extensive 1p-shell studies have been included. The important feature of the A potentials is their strong absorption. This absorption is so strong that essentially all contributions from the nuclear interior are removed and no cutoff is needed to fit the data. However, there is considerable evidence that heavy-ion optical potentials (at least for targets light enough to yield oscillating diffraction patterns at tandem energies) should be much more shallow than those of the Set A.[10-12] Although individual elastic scattering angular distributions can be fitted with deep (i.e., $V \sim 100$ MeV) potentials, studies which have included both energy and angular variations of elastic scattering cross sections have consistently failed to fit the data with deep Woods-Saxon optical potentials. Such studies have included targets in the mass range from ^{12}C through ^{30}Si. Above mass ~30 such systematic studies have not been carried out, but the fixed-energy experiments which have been reported have achieved very successful results with deep potentials.[13,14] It is not clear whether energy-dependence studies would modify this result or whether the marked change in elastic angular distribution shape (from an oscillatory diffraction pattern for $\sigma/\sigma_{\text{Rutherford}}$ to an exponential falloff) for heavy-mass targets at tandem energies indicates the onset of greater ambiguity in the heavy-ion potential. (It may be of interest to note that the best-fit optical potentials for α scattering favor shallow wells when light targets are studied,[15] and in fact there are similarities between the shallow and l-dependent potentials invoked for $\alpha+\alpha$ scattering[16] and for ^{16}O + ^{16}O scattering.[10,12]) Since the targets in the present work span the mass region discussed above, two additional potential sets have been chosen to represent the various types of potential set discussed above. The potential sets B are taken from the ^{28}Si + ^{16}O study of Siemssen *et al.*[11] Since these Sets B have shallow imaginary potentials and correspondingly anomalous mean free paths for the interpenetrating ions and since a previous study has shown that even for light targets there is a continuous W, r_{0i} ambiguity,[17] it would be of interest to modify Set B to include stronger absorption of low partial waves. Present limitations of the code have unfortunately

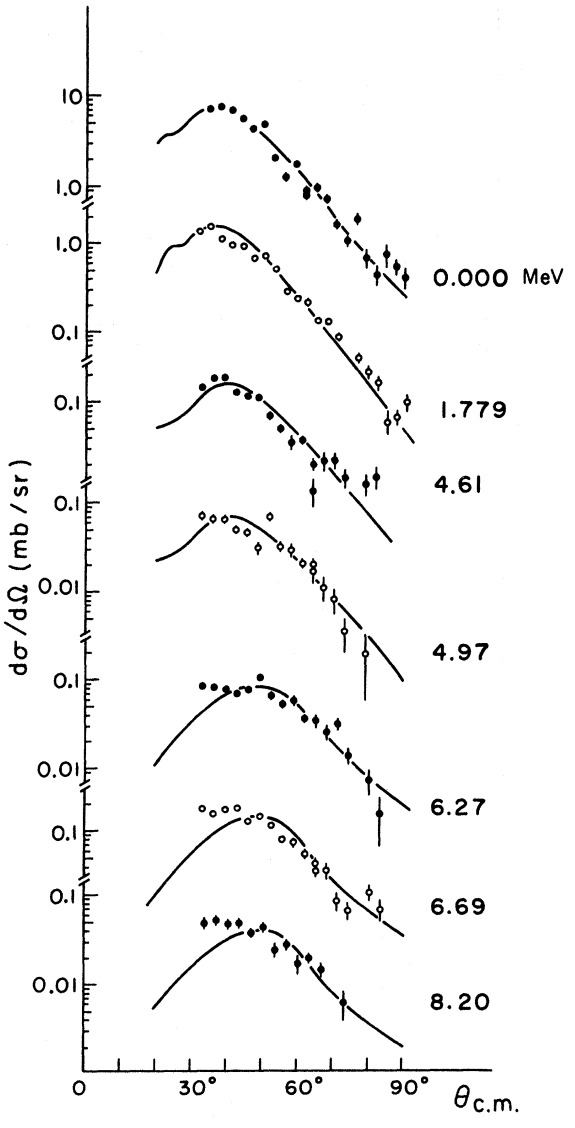

FIG. 4. ^{27}Al(^{16}O, ^{15}N)^{28}Si angular distributions obtained at $E_{^{16}O}$ = 42 MeV. The curves are the results of DWBA calculations using potential set A of Table I.

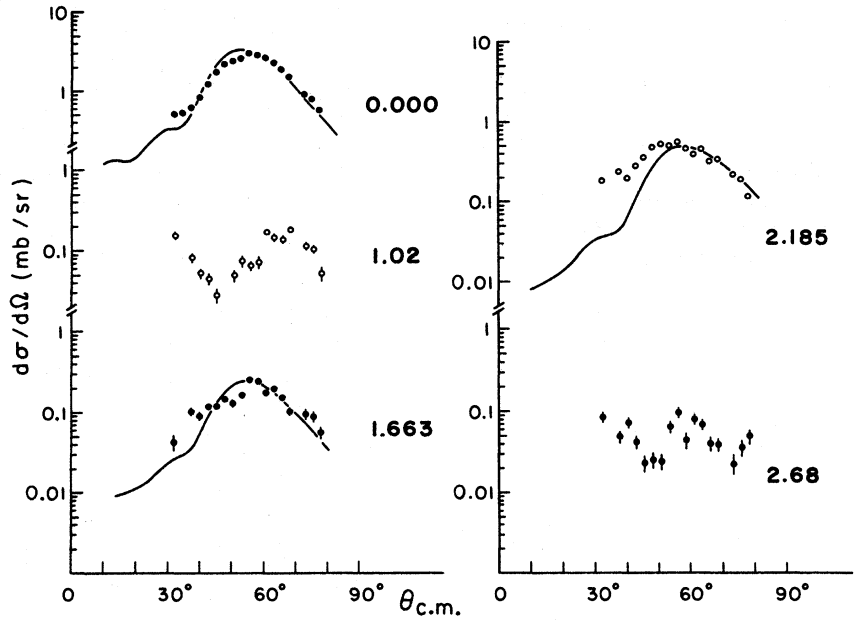

FIG. 5. ^{48}Ti(^{16}O, ^{15}N)^{49}V angular distributions obtained at $E_{^{16}O}$ = 48 MeV. The curves are the results of DWBA calculations using potential set A of Table I.

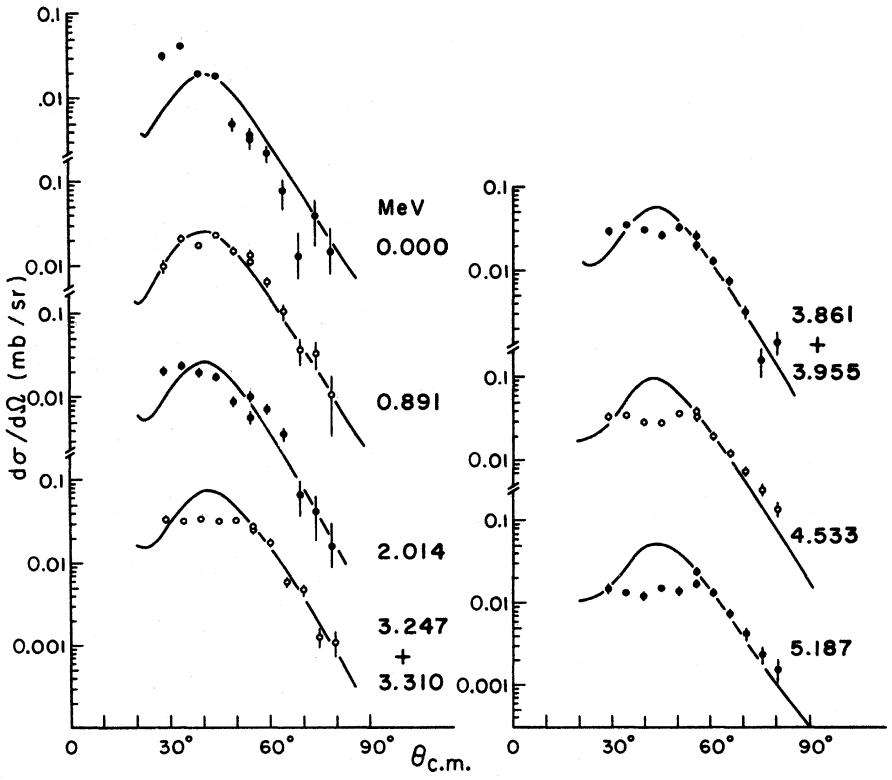

FIG. 6. ^{45}Sc(^{16}O, ^{15}N)^{46}Ti angular distributions obtained at $E_{^{16}O}$ = 53 MeV. The curves are the results of DWBA calculations using potential set A of Table I.

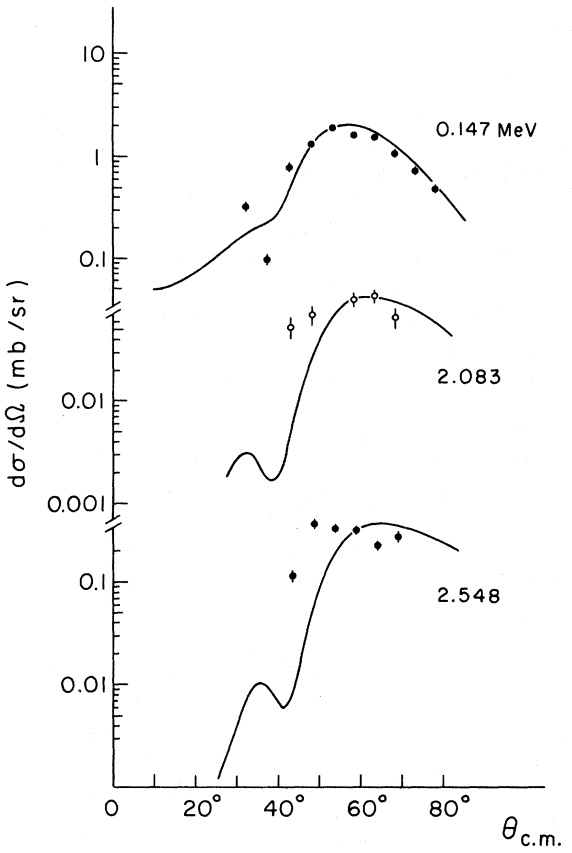

FIG. 7. ^{46}Ti(^{16}O, ^{15}N)^{47}V angular distributions obtained at E_{16_O} = 48 MeV. The curves are the results of DWBA calculations using potential set A listed in Table I.

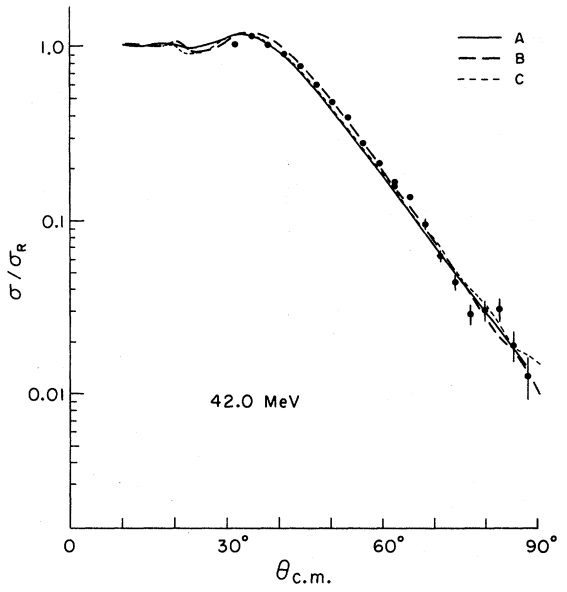

FIG. 8. Comparison of calculated and measured ^{27}Al + ^{16}O elastic scattering angular distributions at E_{16_O} = 42 MeV. Curves A, B, and C were computed using the respective potentials listed in Table I.

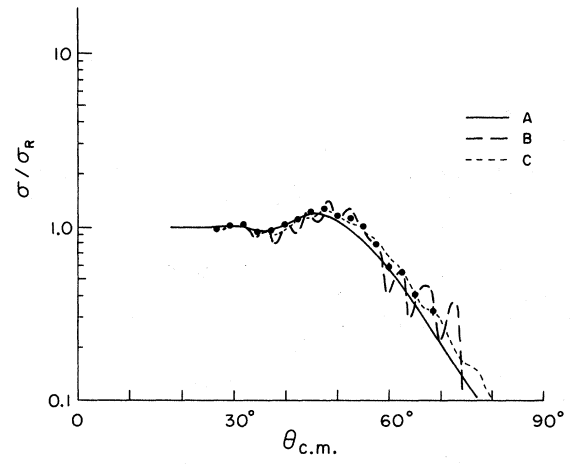

FIG. 9. Comparison of calculated and measured ^{48}Ti + ^{16}O elastic scattering angular distributions at E_{16_O} = 48 MeV. Curves A, B, and C were computed using the respective potentials listed in Table I.

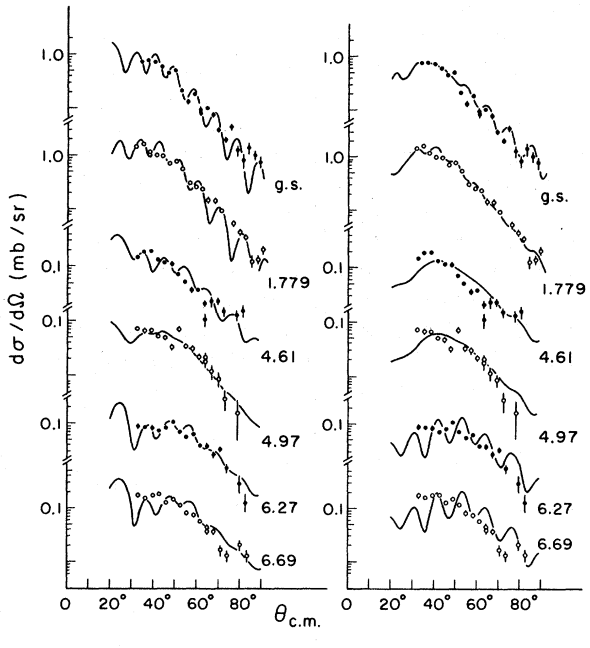

FIG. 10. ^{27}Al(^{16}O, ^{15}N)^{28}Si angular distributions obtained at E_{16_O} = 42 MeV compared with DWBA calculations using the potential sets B (left side of Figure) and C (right side of Figure) listed in Table I.

TABLE I. Optical-model potentials.

	Set	V (MeV)	W (MeV)	r_0 [a] (fm)	a (fm)
^{16}O	A [b]	100.0	40.0	1.22	0.5
	B [c]	14.0	5.0	1.35	0.5
	C(^{16}O+^{27}Al)	60.0	8.02	1.30	0.44
	C(^{16}O+^{48}Ti) [d]	60.2	3.38	1.30	0.4
^{15}N [e]	A	100	40	1.22	0.6
	B	20.5	4.5	1.35	0.6
	C(^{16}O+^{27}Al)	60.0	8.02	1.30	0.5
	C(^{16}O+^{48}Ti)	60.2	3.38	1.30	0.5
p		f	···	1.20	0.65

[a] $R = r_0(A_1^{1/3} + A_2^{1/3})$.

[b] Reference 2.

[c] R. H. Siemssen, Argonne National Laboratory Topical Report No. ANL-7837 (unpublished), p. 145.

[d] Reference 17.

[e] Imaginary diffuseness increased to shift angular distribution maximum as in Ref. 2.

[f] Adjusted to reproduce the experimental binding energies (12.13 MeV for the assumed $p_{1/2}$ proton in ^{16}O, varied in the residual nucleus according to excitation energy.) Spin-orbit effects were not included.

prohibited this. Finally potential sets C are deep potentials derived from a recent study of ^{16}O elastic scattering.[13] Since Morrison *et al.*[2] have found that (^{16}O, ^{15}N) angular distributions are best fitted if the diffuseness of the ^{15}N optical potential is made slightly larger than that of the ^{16}O optical potential, and since such a change is easily accommodated within the present uncertainties regarding ^{15}N potentials, we have increased the diffusenesses of the ^{15}N potentials in Table I by 0.1 fm in each case. No further changes were made in any of the optical parameter sets. The predictions of the oxygen potentials are shown with the elastic scattering angular distributions for ^{27}Al and ^{48}Ti in Figs. 8 and 9. Since these potentials were to be used in an attempt at consistent analysis over the entire mass region studied and since each has already been shown to fit data in this mass region, the potentials were not modified to fit the data in Figs. 8 and 9.

All three potential sets gave acceptable fits to the data shown in Fig. 4. The curves in Figs. 3 and 4 are distorted-wave Born-approximation (DWBA) predictions using Set A. Figure 10 shows fits for the low-lying ^{28}Si states derived from potential sets B and C. As was found by Morrison *et al.*,[2] it was necessary to use a lower cutoff with Sets B or C to fit angular distribution shapes for $1f$-$2p$-shell targets. However, the Q-value effects and relative spectroscopic factors discussed below are very similar for all potential sets. Thus, the systematics of distorted-wave predictions for the (^{16}O, ^{15}N) reaction are not highly sensitive to a choice of optical parameters. For convenience, spectroscopic factors for all three potential sets will be presented only for the ^{27}Al(^{16}O, ^{15}N)^{28}Si reaction (where none needed a lower cutoff) and all further discussion will be limited to results obtained with parameter sets A.

The curves shown in Figs. 5–7 are distorted-wave predictions using optical potentials A and the bound-state-well parameters listed in Table I. Table II lists spectroscopic factors for the ^{27}Al(^{16}O, ^{15}N)^{28}Si angular distributions shown in Fig. 3. Tables III–VI list spectroscopic factors for all states considered in this study, along with the corresponding spectroscopic strengths from other one-proton-stripping reactions which have been reported. Spectroscopic factors from the (^{16}O, ^{15}N) reaction have been extracted using the relation

$$\sigma_{\text{experimental}} = N(C^2S_2)\sum_{\lambda}(C^2S_{1,\lambda})\sigma_{\text{RDRC},\lambda},$$

where $\sigma_{\text{RDRC},\lambda}$ is the prediction of the distorted-wave calculation, C^2S_2 is the spectroscopic factor for the proton bound in ^{16}O (assumed $1p_{1/2}$ with $C^2S_2 = 2$ in all cases), $C^2S_{1,\lambda}$ is the final-state spectroscopic factor listed in Tables II–VI and N is an over-all normalization factor. λ is the orbital angular momentum required to transfer the (assumed) $1p_{1/2}$ proton from the projectile to the configuration (nlj) assumed for the proton in the residual nucleus.

TABLE II. Beam energy dependences of spectroscopic factors extracted from ^{27}Al(^{16}O, ^{15}N)^{28}Si reaction data. Relative values are given in parentheses.

		$\frac{2J_f+1}{2J_i+1}C^2S_1$			
E_x [a]	J^π [a]	36 MeV	42 MeV	48 MeV	53 MeV
0.000	0^+	0.48 (1.0)	0.46 (1.0)	0.41 (1.0)	0.27 (1.0)
1.779	2^+	0.24 (0.51)	0.32 (0.70)	0.23 (0.56)	0.27 (1.0)
4.61	4^+	···	0.14 (0.29)	0.18 (0.45)	···

[a] Taken from P. M. Endt and C. van der Leun, Nucl. Phys. A105, 1 (1967).

TABLE III. Spectroscopic strengths for ^{27}Al(^{16}O, ^{15}N)^{28}Si reaction. The maximum value of $\sigma_{\mathrm{RDRC},\lambda}$ for each excitation energy and assumed configuration is listed in column 4. Relative values are given in parentheses.

E_x [a]	J^π [a]	Assumed configuration	max $\sigma_{\mathrm{RDRC},\lambda}$ (mb/sr)	$\frac{(2J_f+1)}{(2J_i+1)} C^2S_1$ (^{16}O, ^{15}N) [b]		(^{16}O, ^{15}N) [c]		(^{16}O, ^{15}N) [d]		(^{3}He, d) [e]	
0.000	0^+	$1d_{5/2}$	0.036	0.47	(1.0)	0.27	(1.0)	0.32	(1.0)	0.44	(1.0)
1.779	2^+	$2s_{1/2}$	0.55	0.32	(0.69)	0.17	(0.63)	0.23	(0.71)	0.38	(0.86)
4.61	4^+	$1d_{5/2}$	0.22	0.14	(0.30)	0.35	(0.52)	0.11	(0.35)		
		$1d_{3/2}$	0.021	1.92	(4.1)					0.32	(0.73)
4.97	0^+	$1d_{5/2}$	0.23	0.08	(0.16)	0.03	(0.12)	0.05	(0.16)	0.05	(0.11)
6.27	3^+	$2s_{1/2}$	0.023	0.60	(1.28)	0.28	(1.0)	0.50	(1.6)	0.14	(0.32)
										($2s_{1/2}$)	
										0.07	(0.16)
										($1d_{3/2}$)	

[a] Taken from P. M. Endt and C. van der Leun, Nucl. Phys. A105, 1 (1967).
[b] Potential set A.
[c] Potential set B.
[d] Potential set C.
[e] R. W. Barnard and G. D. Jones, Nucl. Phys. A108, 641 (1968).

TABLE IV. Spectroscopic strengths for ^{48}Ti(^{16}O, ^{15}N)^{49}V reaction. The maximum value of $\sigma_{\mathrm{RDRC},\lambda}$ for each excitation energy and assumed configuration is listed in column 3.

E_x [a]	Assumed configuration	max $\sigma_{\mathrm{RDRC},\lambda}$ (mb/sr)	$(2J_f+1)C^2S_1$ (^{16}O, ^{15}N)	(^{3}He, d) [a]	(^{3}He, d) [b]
0.000	$1f_{7/2}$	0.97	3.40	2.5	4.3
1.663	$2p_{3/2}$	0.39	0.33	0.38	0.5
2.185	$1f_{7/2}$	0.40	1.50	0.53	...
	$1f_{5/2}$	0.014	32	...	0.8

[a] D. J. Pullen, B. Rosner, and O. Hansen, Phys. Rev. 166, 1142 (1968).
[b] D. Bachner, R. Santo, H. H. Duhm, R. Bock, and S. Hinds, Nucl. Phys. A106, 577 (1968).

TABLE V. Spectroscopic strengths for the ^{46}Ti(^{16}O, ^{15}N)^{47}V reaction. The maximum value of $\sigma_{\mathrm{RDRC},\lambda}$ for each excitation energy and assumed configuration is listed in column 3.

E_x [a]	Assumed configuration	max $\sigma_{\mathrm{RDRC},\lambda}$ (mb/sr)	$(2J_f+1)C^2S_1$ (^{16}O, ^{15}N)	(^{3}He, d) [a]
0.147	$1f_{7/2}$	0.49	4.3	4.6
2.083	$2p_{3/2}$	0.044	2.4	1.4
2.548	$1f_{7/2}$	0.070	5.4	
	$1f_{5/2}$	0.0011	288	1.4

[a] B. Rosner and D. J. Pullen, Phys. Rev. 162, 1048 (1967).

As discussed in Ref. 7, λ is limited by parity, $(-1)^{1+l+\lambda}=1$, and by the two triangle relationships, $\Delta(1, l, \lambda)$ and $\Delta(\frac{1}{2}, j, \lambda)$. Thus λ is unique for spin-zero targets and is severely limited even for reactions on the odd-mass targets considered below. Spectroscopic factors for the states populated in this study agree best with (^{3}He, d) results if N is taken to be 3.75. This factor is not in good agreement with the value $N=1.5$ found by Morrison *et al.*[2] The source of this disagreement is not understood.

The dominant effect causing the highly selective population of final states seen in this experiment is the angular momentum matching effect (which in turn is closely linked to Q value and only weakly connected with beam energy). This effect can be qualitatively understood in semiclassical terms; i.e., for the (^{16}O, ^{15}N) reaction the individual partial waves in both incoming and outgoing channels are far more localized in space than would be the case for analogous light-ion-induced reactions. This, along with strong absorption in both elastic channels, gives rise to large inhibition factors if angular momentum transfer does not closely triangulate with angular momenta characteristic of grazing trajectories in entrance and exit channels. The most favored angular momentum transfer, λ_{favored}, can be calculated either semiclassically[2] or by comparing Q dependences of distorted-wave calculations. For all cases compared in this study the two methods predict the same value for λ_{favored}. As can be seen from Tables II–VI, the distorted-wave theory gives a sufficiently good account of the angular momentum matching effect to allow reasonable agreement between (^{16}O, ^{15}N) spectroscopic strengths and those extracted from (^{3}He, d) studies. Tables III–VI also include the maximum values of $\sigma_{\text{RDRC},\lambda}$ for each case. Although the aim of this study was not to emphasize spectroscopy, it is of interest to discuss each reaction in some detail in order to focus on the importance of the angular momentum matching conditions and to indicate anomalies that have arisen.

A. ^{27}Al(^{16}O, ^{15}N)^{28}Si

The spectroscopic strengths shown in Table II do not vary significantly with beam energy. The only apparent variation occurs for the ground-state strength at 53 MeV (lab). In this case the angular distribution peaks at small angles where reliable data are extremely difficult to obtain. Thus the process of extracting a strength was sufficiently ambiguous that the deviation from lower-energy values is not considered significant.

The spectrum for this reaction (Fig. 1) shows strong population of the ground state and first excited state of ^{28}Si with much weaker population of higher-lying levels. Orbital angular momentum transfer $\lambda=1$ (appropriate to $1p_{1/2} \rightarrow 2s_{1/2}$ or $1p_{1/2} \rightarrow 1d_{3/2}$ transitions) is least inhibited in the region of the ^{28}Si ground state and becomes very severely inhibited at higher excitation energies. $\lambda=3$ transfer (appropriate to $1p_{1/2} \rightarrow 1d_{5/2}$) is least inhibited

TABLE VI. Spectroscopic strengths for the ^{45}Sc(^{16}O, ^{15}N)^{46}Ti reaction. The maximum value of $\sigma_{\text{RDRC},\lambda}$ for each excitation energy and assumed configuration is listed in column 4.

E_x [a]	J^π [a]	Assumed configuration	max $\sigma_{\text{RDRC},\lambda}$ (mb/sr)	$\frac{2J_f+1}{2J_i+1} C^2S_l$ (^{16}O, ^{15}N)	(^{3}He, d) [a]	(^{3}He, d) [b]	(α, t) [c]
0.000	0^+	$1f_{7/2}$	0.014	0.25	0.53	0.27	0.27
0.891	2^+	$1f_{7/2}$	0.087	0.19	0.96	0.28	0.40
		$2p_{3/2}$	0.43	0.01	0.25	0.06	
2.014	4^+	$1f_{7/2}$	0.18	0.11	0.72	0.22	0.30
		$2p_{3/2}$	0.73	0.02	0.20	0.04	
3.247 +3.310	2^+	$1f_{7/2}$	0.11	0.56	1.14	···	0.55
3.861 +3.955		$1f_{7/2}$	0.15	0.40	0.88	0.36	0.33
		$2p_{3/2}$	0.34	0.04	0.15	0.09	
4.533		$1f_{7/2}$	0.13	0.84	2.11	···	0.76
		$1f_{5/2}$	0.01	11.0			
5.187		$1f_{7/2}$	0.11	0.6	0.17	···	···
		$2p_{3/2}$	0.16		0.02		

[a] Reference 19.
[b] Reference 18.
[c] Reference 20.

at $E_x \sim 3$ MeV and allows significant population of levels up to ~6 MeV excitation. As can be seen in Table III, the strength of the transition to the 4.61-MeV state of ^{28}Si is reasonable if the final orbital is assumed to be $1d_{5/2}$ ($\lambda = 3$), but it would be approximately an order of magnitude too large if a $1d_{3/2}$ configuration were assumed.

It can be seen from Fig. 4 that the calculated angular distributions fit the low-lying levels rather well but show a tendency to predict Q-dependent changes in the *shapes* of the angular distributions which are not borne out by the data. This problem also occurs for reactions on Ti targets. [A different problem of predicting Q dependences of angular distribution shapes arises for the ^{45}Sc(^{16}O, ^{15}N)-^{46}Ti reaction discussed below.]

B. ^{48}Ti(^{16}O, ^{15}N)^{49}V and ^{46}Ti(^{16}O, ^{15}N)^{47}V

The large negative Q values for the ground-state transitions in these reactions lead to the very selective populations of levels evident in the spectra of Fig. 2. For example, in the ^{48}Ti(^{16}O, ^{15}N)^{49}V reaction the ground-state Q value is -5.4 MeV. At this Q value, $\lambda = 4$ (which is appropriate to $1p_{1/2} \rightarrow 1f_{7/2}$) is favored so the ground state is strongly excited. At $E_x = 2$ MeV the favored λ has increased to ~7 (appropriate to no reasonable final shell-model configuration). Thus the 2.185-MeV state in ^{49}V, known from (^{3}He, d) studies (see Table IV) to have a spectroscopic strength about $\frac{1}{5}$ that of the ground state, can be seen in Figs. 2 and 5 to be much more weakly populated than the ground state. The configuration of this 2.185-MeV state could be either $1f_{7/2}$ or $1f_{5/2}$, but the $1f_{5/2}$ assignment is favored because the state is weakly populated in the (t, α) reaction. As can be seen for the (^{16}O, ^{15}N) reaction results shown in Table IV, a very unreasonable spectroscopic factor results from assuming a $1f_{5/2}$ configuration for this state while an assumption of $1f_{7/2}$ appears more reasonable.

Similar arguments hold for states populated in the ^{46}Ti(^{16}O, ^{15}N)^{47}V reaction where the lowest state with large single-particle strength in either (^{3}He, d) or (^{16}O, ^{15}N) is the $\frac{7}{2}^-$ state at 0.147 MeV. As can be seen in Table V, data for the 2.548-MeV level of ^{47}V [which had been assumed to be $\frac{5}{2}^-$ in (^{3}He, d) studies] yield a reasonable spectroscopic factor only if $\lambda = 4$ ($1f_{7/2}$) is assumed.

Two states populated in the ^{48}Ti(^{16}O, ^{15}N)^{49}V reaction have angular distributions (Fig. 5) which cannot be fitted with distorted-wave calculations. These are assumed to be populated through some higher-order process. Evidence has been seen for the population of a known low-lying $\frac{11}{2}^-$ state in the ^{50}Ti(^{16}O, ^{15}N)^{51}V reaction and attempts have been made to explain this observation in terms of multistep reaction mechanisms.[2,4] Unfortunately, the spectroscopy of ^{49}V is not sufficiently well known to justify further analysis of the states seen in this study. Evidence for the population of some very weak states in ^{47}V can be seen in the spectrum for the ^{46}Ti(^{16}O, ^{15}N)^{47}V reaction (Fig. 2), but it has not been possible to extract angular distributions from these small cross sections.

C. ^{45}Sc(^{16}O, ^{15}N)^{46}Ti

The ground-state Q value (-1.78 MeV) for this reaction allows population of states over a relatively large range of excitation energy in ^{46}Ti. $\lambda = 0$ should be dominant at the ground-state Q value, while $\lambda = 4$ should be most favored at $E_x \sim 4$ MeV. It can be seen from the spectrum (Fig. 1) and from the peak cross sections of the angular distributions that the most strongly favored transitions lie in the range ~2 MeV $\leq E_x <$ ~5 MeV. The distorted-wave calculations could not reproduce the marked flattening of the angular distribution maxima with increasing Q value. For this reason, the DWBA predictions were normalized to the (approximately) exponential falloff of the angular distributions at larger angles. The resulting spectroscopic strengths, seen in Table VI, are in good agreement with results of (^{3}He, d) and (α, t) studies.[18-20] One point requires further discussion. The 0.891- and 2.014-MeV levels are known to be populated by mixed $2p_{3/2}$ and $1f_{7/2}$ transfer in (^{3}He, d) studies.[18,19] These configurations require $\lambda = 2$ and $\lambda = 4$, respectively, in the (^{16}O, ^{15}N) reaction, but angular momentum matching results in considerable enhancement of $\lambda = 2$. These transitions produce angular distributions with very similar shapes in the present work so that empirical separation of the two is impossible. Therefore in the analysis of each of these transitions, the ratios of strengths from light-ion-induced reactions were assumed to be roughly correct and arbitrary divisions of (^{16}O, ^{15}N) cross section were made to give best agreement in Table VI.

D. ^{24}Mg(^{16}O, ^{15}N)^{25}Al and ^{28}Si(^{16}O, ^{15}N)^{29}P

These reactions both have very large negative Q values. In each case the distorted-wave theory predicts peak cross sections smaller than 10 μb/sr for the strongest single-particle states that could be populated. Observed yields (~10 events) at expected peak angles are in qualitative agreement with this prediction. These reactions are so inhibited by angular momentum mismatch effects [the favored angular momentum transfer for the ^{24}Mg(^{16}O, ^{15}N)^{25}Al ground-state transition is $\lambda = 8$, while the required $1p_{1/2} \rightarrow 1d_{5/2}$ transfer can only

proceed *via* $\lambda = 3$] that no angular distributions could be extracted for any final state in either reaction.

V. SUMMARY AND CONCLUSIONS

The (^{16}O, ^{15}N) reaction has been studied on targets of ^{24}Mg, ^{27}Al, ^{28}Si, ^{45}Sc, and ^{46,48}Ti and finite-range distorted-wave calculations have accounted well for the extreme Q dependences of the cross sections, yielding spectroscopic factors in good agreement with spectroscopic factors extracted from light-ion-induced reactions. Thus, the results of this study and of similar studies indicate that the distorted-wave theory gives a satisfactory account of the systematics of the (^{16}O, ^{15}N) reaction. The dominant systematic which gives rise to the selectivity of this reaction is a strong dependence on angular momentum matching. To a considerable extent these heavy-ion reactions can be understood in semiclassical terms: The individual partial waves in both incoming and outgoing channels are far more localized in space than would be the case for analogous light-ion-induced reactions and this coupled with strong absorption in both elastic channels gives rise to large inhibition factors if angular momentum transfer does not closely triangulate with angular momenta characteristic of grazing trajectories in entrance and exit channels. Thus this angular momentum matching consideration, which occasionally can be an important factor in transfer reactions induced by light ions, becomes the dominant effect for the (^{16}O, ^{15}N) reaction. The agreement of spectroscopic factors listed in Tables III–VI, despite the wide range in absolute cross sections shown in Figs. 6–9 exhibits the success of the DWBA in accounting for this effect.

The picture that emerges from the present study, as well as from early heavy-ion-induced proton-stripping studies on targets in the $1p$ shell,[3] and from other recent work in the $1f$-$2p$ shell,[2,4] indicates that these reactions are sufficiently uncontaminated by the many possible complications which could in principle arise in the interactions of two complex nuclei that the distorted-wave theory accounts well for their systematics over a wide range of target mass, angular momentum transfer, and Q value. Additional (^{16}O, ^{15}N) experiments will be needed to test these conclusions further, but it is also of interest to attempt to extend the theory to include large-cluster-transfer reactions. Indeed, recent studies are beginning to provide the data needed for such work.[1,2,4,21] If systematics of larger cluster transfer do become evident empirically, it may become possible to proceed with some confidence to the study of nuclear phenomena which are not accessible with standard light-ion-induced reaction techniques.

ACKNOWLEDGMENTS

We are grateful to Dr. W. R. Tobocman for making his distorted-wave code RDRC available to us. We are indebted to Dr. R. H. Siemssen for helpful discussions. The help of Dr. J. J. Kolata with the on-line data-acquisition system is also gratefully acknowledged.

---

*Work supported by the National Science Foundation.

[1] J. V. Maher, K. A. Erb, G. H. Wedberg, J. L. Ricci, and R. W. Miller, Phys. Rev. Letters 29, 291 (1972); J. V. Maher, R. Miller, and K. A. Erb, Bull. Am. Phys. Soc. 16, 1148 (1971); R. Miller, J. V. Maher, and K. A. Erb, *ibid.* 16, 1148 (1971); K. A. Erb, R. Miller, and J. V. Maher, *ibid.* 16, 1148 (1971); G. H. Wedberg, K. A. Erb, R. Miller, J. Ricci, and J. V. Maher, *ibid.* 17, 530 (1972).

[2] G. C. Morrison, H. J. Korner, L. R. Greenwood, and R. H. Siemssen, Phys. Rev. Letters 28, 1662 (1972); G. C. Morrison, J. Phys. C Suppl. 11-12 32, 6 (1971).

[3] U. C. Schlotthauer-Voos, H. G. Bohlen, W. von Oertzen, and R. Bock, Nucl. Phys. A180, 385 (1972); M. Liu, W. von Oertzen, J. C. Jacmart, F. Pougheon, M. Riou, J. C. Roynette and C. Stephan, Nucl. Phys. A165, 118 (1971); W. von Oertzen, H. H. Gutbrod, U. C. Voos and R. Bock, Nucl. Phys. A133, 101 (1969), and references therein.

[4] H. Faraggi, M. C. Lemaire, J. M. Loiseaux, M. C. Mermaz, and A. Papineau, Phys. Rev. C 4, 1375 (1971), and references therein.

[5] E. Newman, K. S. Toth, and A. Zucker, Phys. Rev. 132, 1720 (1963).

[6] A. Dar, Phys. Rev. 139, B1193 (1965); W. E. Frahn and R. H. Venter, Nucl. Phys. 59, 651 (1964), and references therein.

[7] F. Schmittroth, W. Tobocman, and A. A. Golestaneh, Phys. Rev. C 1, 377 (1970).

[8] P. J. A. Buttle and L. J. B. Goldfarb, Nucl. Phys. A176, 299 (1971).

[9] U. C. Voos, W. von Oertzen, and R. Bock, Nucl. Phys. A135, 207 (1969), and references therein.

[10] J. V. Maher, M. W. Sachs, R. H. Siemssen, A. Weidinger, and D. A. Bromley, Phys. Rev. 188, 1665 (1969); W. Reilly, R. Wieland, A. Gobbi, M. W. Sachs, and D. A. Bromley, in *Proceedings of the International Conference on Nuclear Reactions Induced by Heavy Ions*, edited by R. Bock and W. R. Hering (North-Holland, Amsterdam), p. 93; W. Reilly, R. Wieland, A. Gobbi, M. W. Sachs, J. V. Maher, D. Mingay, R. H. Siemssen, and D. A. Bromley, *ibid.*, p. 95.

[11] G. C. Morrison, H. T. Fortune, and R. H. Siemssen, in *Proceedings of the International Conference on Nucle-*

ar Reactions Induced by Heavy Ions (see Ref. 10), p. 72; H. T. Fortune, A. Richter, R. H. Siemssen and J. W. Tippie, *ibid.*, p. 69; R. H. Siemssen, H. T. Fortune, R. Malmin, A. Richter, J. W. Tippie, and P. P. Singh, Phys. Rev. Letters 25, 536 (1970); G. C. Morrison, H. T. Fortune and R. H. Siemssen, Phys. Rev. C 3, 2133 (1971).

[12]R. A. Chatwin, J. S. Eck, D. Robson, and A. Richter, Phys. Rev. C 1, 795 (1970).

[13]J. Orloff and W. W. Daehnick, Phys. Rev. C 3, 430 (1971).

[14]E. H. Auerbach and C. E. Porter, in *Proceedings of the Third Conference on Reactions Between Complex Nuclei, Asilomar, Pacific Grove, California, 1963,* edited by A. Ghiorso, R. M. Diamond, and H. E. Conzett (Univ. of California Press, Berkeley, 1963), p. 19.

[15]L. McFadden and G. R. Satchler, Nucl. Phys. 84, 177 (1966).

[16]M. W. Kermode, Nucl. Phys. A104, 49 (1967), and references contained therein; S. Ali and A. R. Bodner, Nucl. Phys. 80, 99 (1966).

[17]J. V. Maher, R. H. Siemssen, M. W. Sachs, A. Weidinger, and D. A. Bromley, in *Proceedings of the International Conference on Reactions Between Complex Nuclei, Heidelberg, 1969,* edited by R. Bock and W. R. Heinz (North-Holland, Amsterdam, 1970), p. 60.

[18]R. W. Barnard and G. D. Jones, Nucl. Phys. A111, 17 (1968).

[19]L. Broman and D. J. Pullen, Nucl. Phys. A110, 161 (1968).

[20]J. R. Priest and J. S. Vincent, Phys. Rev. 182, 1121 (1969).

[21]R. H. Siemssen, M. L. Halbert, M. Saltmarsh, and A. van der Woude, Phys. Rev. C 4, 1004 (1971); R. H. Siemssen, C. L. Fink, L. R. Greenwood, and H. J. Korner, Phys. Rev. Letters 28, 626 (1972); G. J. Wozniak, H. L. Harney, K. H. Wilcox, and J. Cerny, Phys. Rev. Letters 28, 1278 (1972); C. Chasman, S. Cochavi, M. J. LeVine, and A. J. Schwarzschild, Phys. Rev. Letters 28, 843 (1972).

PHYSICAL REVIEW C VOLUME 7, NUMBER 2 FEBRUARY 1973

^{13}C States via the ^{12}C$(d, p)^{13}$C Reaction*

J. D. Goss, A. A. Rollefson, G. L. Marolt, and C. P. Browne
Department of Physics, University of Notre Dame, Notre Dame, Indiana 46556
(Received 16 October 1972)

Protons from the ^{12}C$(d, p)^{13}$C reaction were analyzed with a magnetic spectrograph. Bombarding energies ranged from 14.0 to 15.5 MeV and observation angles ranged from 20 to 120°. Eight states were found in ^{13}C between 10.7- and 12.2-MeV excitation energy. Excitation energies and (widths) in keV are: 10 755 ± 5 (56 ± 2), 10 818 ± 5 (24 ± 3), 10 997 ± 8 (82 ± 15), 11 080 ± 5 (<8), 11 748 ± 10 (107 ± 14), 11 851 ± 5 (68 ± 4), 11 970 ± 40 (~260), and 12 108 ± 5 (81 ± 8). The level at 11 851 has not been reported before. Uncertainties in excitation energies are reduced by as much as a factor of 4 from previous work.

I. INTRODUCTION

The purpose of the present work is to provide accurate positions and widths for states in ^{13}C in the 10.5- to 12.2-MeV region of excitation. Although many reactions have been used previously to investigate this region, a glance at a compilation of nuclear data[1] shows that in most cases, excitation energies are not known to better than 20 keV and the widths are quite uncertain and are in many cases only estimates. States above 10.651 MeV are unbound to α as well as neutron emission and a major difficulty with any investigation of the region is that levels overlap and all but one have widths between 20 and 300 keV. Spectra from reactions that leave ^{13}C as the residual nucleus are usually complicated by the presence of contaminant groups which either obscure the broad levels or make analysis of the data difficult. Although contaminants are not usually a serious problem in reactions which have ^{13}C as the compound nucleus, the determination from resonance data of accurate widths and positions in a complicated energy spectrum can be difficult. In the present work the ^{12}C$(d, p)^{13}$C reaction was chosen since targets can be made with few contaminants, thus allowing relatively "clean" proton spectra to be obtained. Because of the complicated energy spectrum, we determined positions and widths of the levels by fitting the proton spectra with an incoherent sum of simple Breit-Wigner resonances plus a quadratic background term. The results of this analysis are discussed and presented below.

II. EXPERIMENTAL

Self-supporting natural carbon targets were made from 20- and 40-μg/cm^2 commercial carbon foils. Deuteron beams were produced with the University of Notre Dame FN tandem Van de